Preparation of Highly Active Silica-Supported Au Catalysts for CO Oxidation by a Solution-Based Technique

Haoguo Zhu, Chengdu Liang, Wenfu Yan,† Steven H. Overbury, and Sheng Dai*

Chemical Sciences Division, Oak Ridge National Laboratory, Oak Ridge, Tennessee 37831

Received: January 30, 2006; In Final Form: April 12, 2006

Although Au catalysts can be readily prepared on titania via the deposition−precipitation (DP) method, the direct application of the method similar to the preparation of silica-supported Au catalysts only results in diminished success. This paper reports a novel, efficient method to synthesize highly active Au catalysts supported on mesoporous silica (SBA-15) through a gold cationic complex precursor $[Au(en)_2]^{3+}$ (en = ethylenediamine) via a wet chemical process. The gold cationic precursor was immobilized on negatively charged surfaces of silica by a unique DP method that makes use of the deprotonation reaction of ethylenediamine ligands. The resulting mesoporous catalyst has been demonstrated to be highly active for CO oxidation at room temperature and even below 273 K, the activity of which is much superior to that of silica-supported Au catalysts previously prepared by various solution techniques. The pH value of the gold precursor solution plays a key role in determining the catalytic activity through the regulation of $[Au(en)_2]^{3+}$ deprotonation reaction and the surface interaction of silica with the gold precursor. This mesoporous gold silica catalyst has also been shown to be highly resistant to sintering because of the stabilization of Au nanoparticles inside mesopores.

Introduction

Since supported Au nanoparticles between 2 and 5 nm were demonstrated to be extremely active catalysts for CO oxidation in late 1980s,[1,2] the gold nanoparticles deposited on metal oxides, such as Al_2O_3, TiO_2, CeO_2, ZrO_2, MgO, Fe_2O_3, etc., have been extensively studied,[3−7] giving evidence of their activity dependence on the size of Au particles and on the nature of supports. Highly dispersed Au nanoparticles are usually prepared by a liquid-phase deposition−precipitation (DP) method.[8] Auric acid ($HAuCl_4$) is usually used as an inexpensive gold precursor to deposit $Au(OH)_3$ on the surfaces of oxides. The DP procedure involves the adjustment of the pH value of $HAuCl_4$ solution to 6−10 for generation of surface-reactive gold hydroxide species.[9,10] The prerequisite for the incorporation of such Au(III) precursors requires the interaction of the anionic $Au(OH)_xCl_{4-x}^-$ complexes with a positively charged oxide surface.[11] Accordingly, the isoelectric point (IEP) of the support matrix plays a key role for the successful incorporation and dispersion of gold precursors into the corresponding oxide support. The oxides with high IEPs, such as titanium oxide (IEP ≈ 6.0), are favored in this aqueous DP synthesis. The isoelectric point of silica is relatively low (∼2), implying that the surface of silica is highly negatively charged under the DP conditions. Therefore, the direct DP and coprecipitation methods are difficult to be used for preparing gold catalysts supported on silica through the $HAuCl_4$ precursor.[3,8]

To date, few reports concerning gold deposited on silica have shown good catalytic activities even though several methods to synthesize small gold particles on silica have been published.[12,13] Therefore, silica is usually considered to be ineffective as a support for the dispersion of gold in a catalytically active form.[14−19] However, Haruta et al.[20] have recently employed a chemical vapor deposition (CVD) methodology using an expensive organometallic gold precursor to obtain silica-supported gold particles that were small enough (mean size ca. 6.6 nm) to be active for CO oxidation even at temperature lower than 273 K.[20] The CVD process involves more sophisticated apparatus and is difficult to adapt to the large-scale preparation of powdered catalysts. Nevertheless, the observed high catalytic activity does indicate that silica can be regarded as a good support for catalytically active gold nanoparticles. The previous unsuccessful attempts to incorporate gold catalysts into silica via the DP method can be attributed to the limited choice of gold precursors.

To the best of our knowledge, the deposition of gold nanoparticles with high dispersion and high catalytic activity using inexpensive solution-phase precursors (e.g., $HAuCl_4$) on silica surfaces has not been achieved.[12,13] This deficiency results from the tendency of the gold hydroxide species toward agglomeration on silica surfaces because of the weak surface interaction provided by negatively charged silica surfaces. Especially in solution phase, this weak interaction of the gold precursor species with silica surfaces is accompanied by redox reactions under basic conditions.[21] The reduced gold nanoparticles provide the "catalytic" seeds for the uncontrolled aggregation of the gold species. To overcome the weak interaction of the gold species with silica surfaces, we[22] and other groups[14,23] have developed a silica-surface modification scheme, the essence of which is to form Au(III) complexes with bifuctional ligands through dative bonds. The controlled growth of Au nanoparticles on mesoporous surfaces was achieved by mild chemical reduction. The drawbacks associated with this strategy are three-fold: (1) no direct interaction of Au(III) ions with silica surfaces, (2) the retention of chloride ions during

* To whom correspondence should be addressed. Telephone: (865) 576-7307. Fax: (865) 576-5235. E-mail: dais@ornl.gov.

† Present address: State Key Laboratory of Inorganic Synthesis and Preparative Chemistry, College of Chemistry, Jilin University, Changchun 130012, P. R. China.

10.1021/jp060637q CCC: $33.50
Published on Web 05/12/2006

TABLE 1: Particle Size, Au Loading, and Residual Chloride of the Gold Catalysts Synthesized Using the Same $Au(en)_2Cl_3$ Precursor Concentration under Different pH Values

sample[a]	final pH in synthesis	Au loading (wt %)	Cl (ppm)	Cl/Au (molar ratio)	Mean diameter of Au (nm)	
					D_{XRD}[b]	D_{TEM}[c]
SBA-15-pH-6-A-C400	6.0	2.70	34	0.07	4.4	5.4
SBA-15-pH-7.4-A-C400	7.4	5.98	43	0.04	4.0	5.2
SBA-15-pH-8.5-A-C400	8.5	6.90	32	0.03	3.7	4.9
SBA-15-pH-9.6-A-C400	9.6	9.08	–	–	3.7	4.9

[a] A-C400: activated at 673 K. [b] D_{XRD}, determined by XRD. [c] D_{TEM}, observed by TEM.

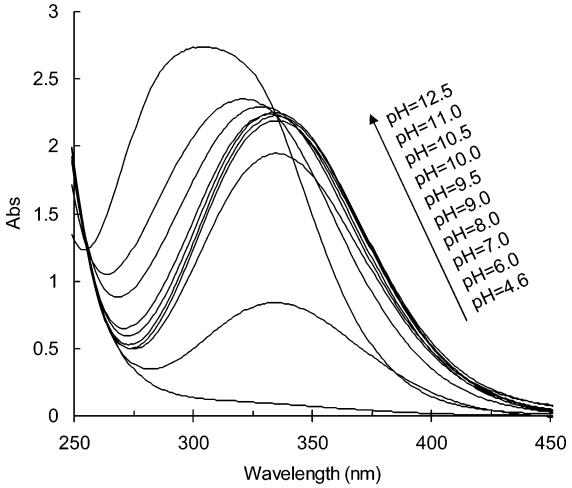

Figure 1. UV−vis spectra of a gold solution (1.5 mM) at different pH values (indicated above each spectrum).

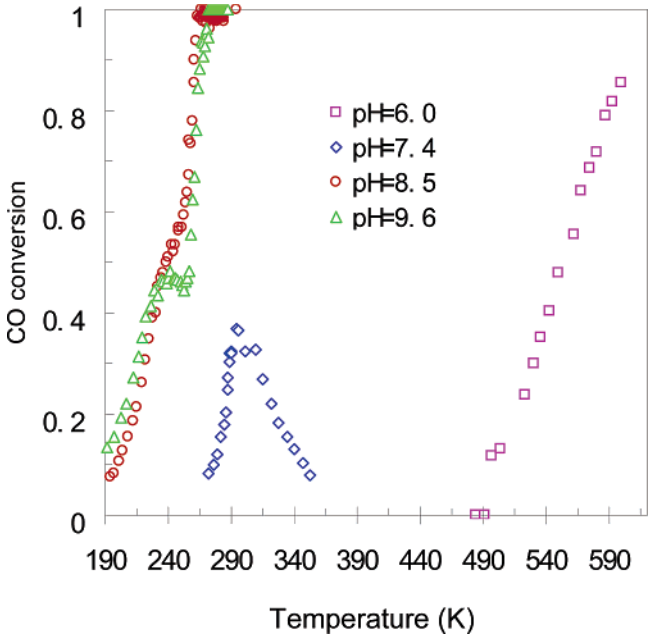

Figure 2. Light-off curves of the Au catalysts supported on SBA-15, synthesized in the solutions of $Au(en)_2Cl_3$ with different pH values.

deposition, and (3) the necessity to remove large amounts of organic functional groups on silica surfaces during post high-temperature treatments. All these deficiencies affect the development of the strong metal−support interaction (SMSI), which may be the key to stabilize active gold catalysts. Therefore, the Au catalysts prepared by this surface-modification method are usually inactive below 373 K.[14−16] It is still a synthesis challenge to prepare active silica-supported Au catalysts at room temperature by a solution-based method.

Herein, we reported an efficient method to synthesize silica-supported highly active Au catalysts through DP of a gold cationic complex precursor ($[Au(en)_2]^{3+}$, en = ethylenediamine). Although the cationic complex precursor has been used to prepare gold catalysts on silica by cationic exchange,[12,24,25] only limited catalytic activities were reported. Our research to develop new methodologies to prepare highly active silica-supported catalysts was also motivated by the beneficial properties of silica materials, such as ease to control mesopore structures and high-temperature stability. A unique DP method mediated via a coordination complex precursor was developed to immobilize the cationic precursor on the negatively charged surface of silica. The gold nanoparticles in mesoporous silica were subsequently generated by reduction under H_2 atmosphere. The resulting Au catalyst exhibits an extremely high catalytic activity for CO oxidation even below 273 K.

Experimental Section

1. Synthesis of Mesoporous Silica (SBA-15).[26] In a typical run, 16 g of P123 and 120 g of 2 M HCl solution were mixed. The resulting mixture was stirred at 308 K to obtain a clear solution, to which 480 g of water and 34 g of tetraethyl orthosilicate (TEOS) were gradually added. A white precipitate gradually formed. Subsequently, the gel solution was transferred to an autoclave, undergoing hydrothermal treatment at 373 K for 24 h. The as-synthesized SBA-15 was obtained by filtration, washing, drying, and calcination at 823 K.

2. Synthesis of $Au(en)_2Cl_3$.[27] Typically, 0.45 mL of ethylenediamine (en) was slowly added to the aqueous solution of $HAuCl_4 \cdot 3H_2O$ (1.0 g in 10.0 mL of H_2O) until a transparent brown solution was formed. This solution was stirred for 30 min. Subsequently, 70.0 mL of ethanol was added. A precipitation was immediately produced. The final product was filtered, washed by ethanol, and dried overnight in a vacuum oven at 313 K.

3. Synthesis of Gold Catalysts on SBA-15. Typically, 0.372 g of $Au(en)_2Cl_3$ was dissolved in 150 g of H_2O. The pH value of the above solution was adjusted to 10.0 by addition of a NaOH solution (5.0 wt %). Subsequently, 2.0 g of the as-synthesized SBA-15 was added. The pH value of the solution decreased immediately, and the final pH value was controlled between 6 and 10.0 by the further addition of the NaOH solution. The mixed solution was stirred for an additional 2 h. The pH value of the solution was recorded before filtration. The final product was dried at a vacuum oven for 2 days. The yellowish product was then reduced by flowing H_2/Ar (4.0%) at 423 K for 1 h.

4. Catalyst Characterization. Powder X-ray diffraction (XRD) data were collected via a Siemens D5005 diffractometer with Cu Kα radiation ($\lambda \approx 1.5418$ Å). The surface areas and pore structures of catalysts were characterized using a nitrogen adsorption−desorption measurement (Autosorb-1, Quantachrome). The pH value of solutions was adjusted by QC-Titrate (Man-Tech Associates Inc). Both bright-field and dark-field (Z-contrast) transmission electron microscopy (TEM) investigations were carried out using an HD-2000 scanning transmission

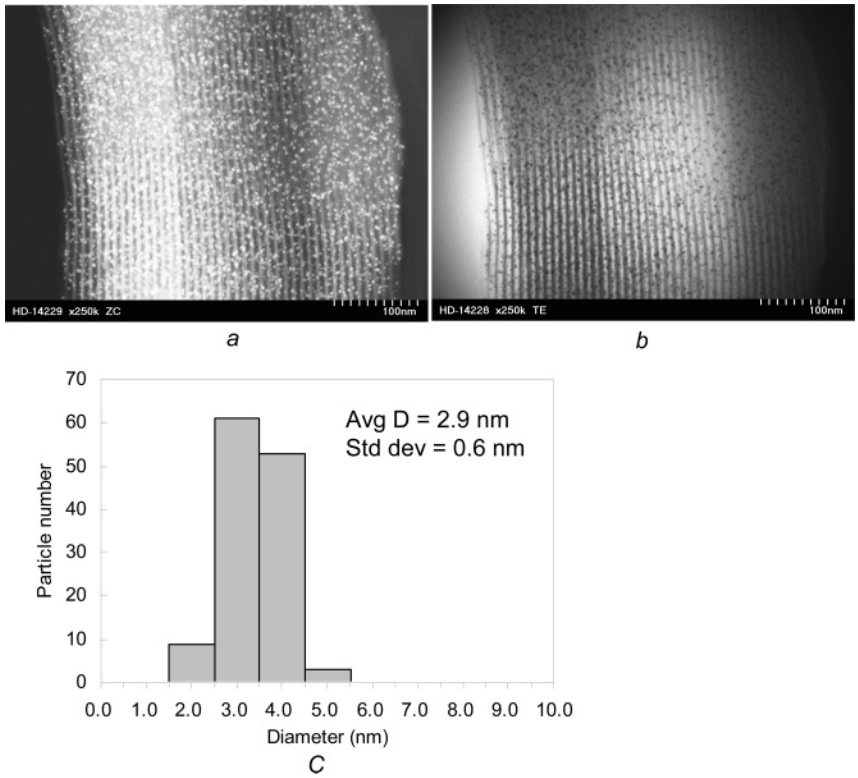

Figure 3. TEM images [(a) dark field and (b) bright field] of the Au catalyst supported on SBA-15 (synthesized at pH of 9.6 and reduced at 423 K) and the corresponding particle-size distribution (c).

electron microscopy (STEM) operated at 200 kV. Inductively coupled plasma (ICP) analysis was performed on an IRIS Intrepid II XSP spectrometer (Thermo Electron Corporation). UV−vis spectroscopic measurements were carried out on a UV−visible spectrophotometer (Cary 4E, Varian). Thermogravimetric analysis (TGA) was recorded on a TGA 2950 (TA Instruments) instrument using a heating rate of 10 °C/min in air.

5. Catalytic Test: CO Oxidation. Prior to a catalysis test, each catalyst was activated by calcination in an oven under air at 673 K for 1 h. Subsequently, the catalytic oxidation of carbon monoxide was carried out in an AMI 200 (Altamira Instruments). Typically, 50 mg of a selected catalyst was packed into a 4 mm i.d. silica U-tube and supported by quartz wools. Without pretreatment, the CO conversion of the sample was measured as a function of temperature (light-off curve). A gas stream of 1% CO balanced with dry air (<4 ppm water) was flowed at ambient pressure through the catalyst at a rate that was adjusted from sample to sample to maintain a constant space velocity of 44 400 mL/(h·g catalyst) or about 37 cm^3/min. The gas exiting the reactor was analyzed by a Buck Scientific 910 gas chromatograph equipped with a dual molecular sieve/porous polymer column (Alltech CTR1) and a thermal conductivity detector. For thermal stability tests, a sample pretreatment was carried out on the same instrument using premixed 8% O_2−He at 773 K (heating rate: 30 °C/min) and holding for 1−4 h. The reaction temperature was varied by using an oven or by immersing the U-tube reactor in a Dewar of ice water or liquid nitrogen-cooled acetone, which slowly warmed throughout the approximately 10−20 h taken to measure a light-off curve. The gold particle size of the final catalysts was characterized by STEM. No significant changes of the catalytic activities for the calcined catalysts stored at the ambient temperature were observed during a 15-day stability test.

Results and Discussion

As mentioned before, the most effective method developed to date for preparation of Au catalysts supported on titanium oxide and other metal oxides is the DP synthesis using an auric acid aqueous solution as a gold precursor.[8] As pointed out earlier, the low IEP of silica prevents the direct application of the DP method in depositing Au species on silica surfaces. The objective of our current investigation is to explore the use of a ligand-exchange reaction to change the charge and thereby the surface-interaction properties of Au precursors. The ligand used in this investigation is ethylenediamine, which is known to form highly stable cationic complexes with Au(III) through the displacement of inner-sphere chloride ligands in $[AuCl_4]^-$. The positive $[Au(en)_2]^{3+}$ ions can readily undergo ion-exchange reactions with cationic surface species on silica. The general reaction mechanism can be expressed as in eq 1, where (Si−O^-) is a surface anionic group on silica surfaces, M^{+1} a singly charged cation interacted with anionic silica surfaces.[28,29] This cation-exchange reaction has been demonstrated before to introduce cationic gold species onto oxide surfaces.[24,25]

$$[Au(en)_2]^{3+} + 2Cl^- + M^{+-}OSi\equiv \rightarrow M^+(aq) + [Au(en)_2Cl_2]^{+-}OSi\equiv \quad (1)$$

$$[Au(en)(d\text{-}en)]^{2+} + Cl^- + M^{+-}OSi\equiv \rightarrow M^+(aq) + [Au(en)(d\text{-}en)Cl]^{+-}OSi\equiv \quad (2)$$

[d-en = deprotonated ethylenediamine ligand ($NH_2CH_2CH_2$-NH^-)].

It is known that the high positive charge density of Au (III) can enhance the acidity of the ethylenediamine ligand and the proton connected to the amine group of ethylenediamine can be easily deprotonated under basic conditions.[27] A study of the behavior concerning the $Au(en)_2Cl_3$ solution at different pH was

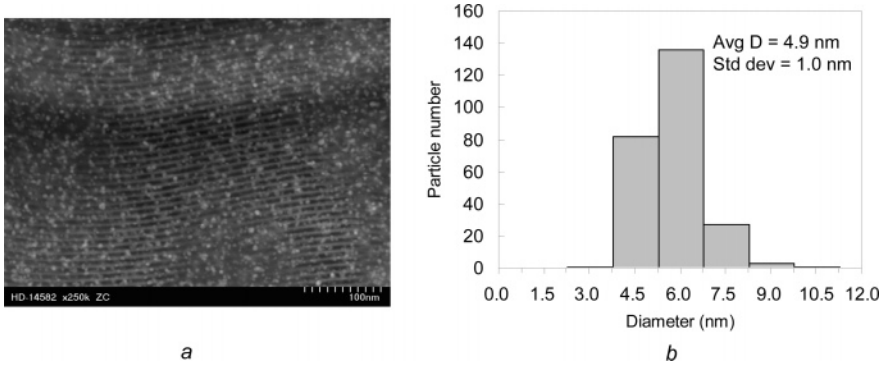

Figure 4. Dark-field TEM images of Au supported on SBA-15 and activated at 673 K (synthesized at pH of 9.6) after catalytic testing (a) and particle size distribution (b).

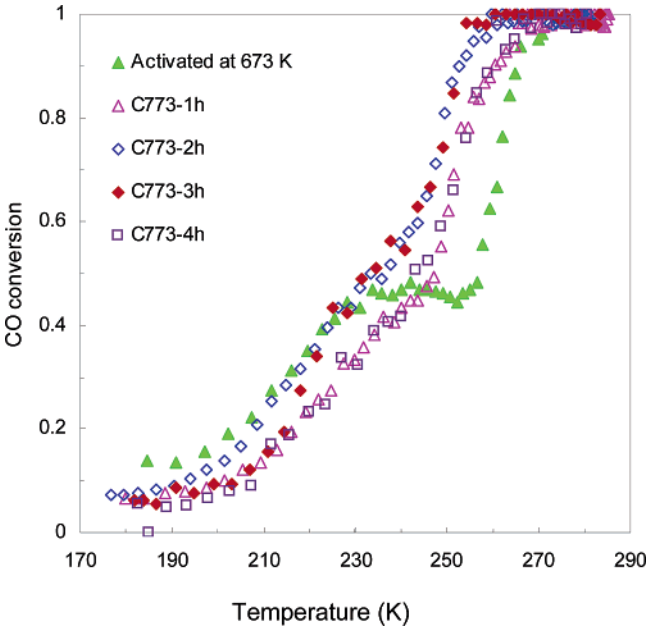

Figure 5. Light-off curves of the Au catalyst supported on SBA-15, calcined at 773 K from 1 to 4 h after activation at 673 K (synthesized at pH of 9.6).

undertaken. Figure 1 shows that a new absorption band at 334 nm increases with the pH value of the $Au(en)_2Cl_3$ solution. The appearance of the absorption band at 334 nm could be correlated to the transformation of the square-planar $Au(en)_2^{3+}$ cation to a pseudo-octahedral complex through the partial formation of the axial dative bonding with hydroxide anions.[30,31] The further increase of pH resulted in the high-energy shift of the absorption band from 334 to 304 nm (pH $\approx$ 12.5) with the concomitant increase of the absorbance. In the titration of $Au(en)_2Cl_3$ with dilute sodium hydroxide, one equivalent of sodium hydroxide was consumed per gold atom, and the solution changed from colorless to yellow (see Figure 1s). This observation supports that one hydrogen from the $Au(en)_2^{3+}$ cation is deprotonated above pH of 8.0.[27] Accordingly, the yellow compound can be assigned to $[Au(en)(d\text{-}en)L]^+$ (L = Cl^- or OH^-), in which (d-en) represents the deprotonated ethylenediamine molecule, i.e., $NH_2CH_2CH_2NH^-$.[27,31] Chloride ions could be further displaced by hydroxide groups with the increase of pH. The concentration of the deprotonated gold cationic complexes also increases with pH. Above pH of 8.0, the dominant DP species are the deprotonated cationic complexes instead of $Au(en)_2^{3+}$. These deprotonated gold cationic complexes are the key to the high catalytic activities observed for the gold catalysts prepared under high pH conditions (vide infra).

The gold loading via the DP method through a cationic gold precursor is proportional to the surface concentration of ($Si-O^-$), which increases with pH of the deposition solution. Therefore, the deposition of Au(III) can be more readily achieved at the pH value significantly higher than the IEP value of the supporting oxide in the DP method using cationic gold complex precursors. This assertion is consistent with our experimental observation, which shows that the Au loading increases with pH as shown in Table 1. The low IEP value of SiO_2 limits the application of the conventional DP with $AuCl_4^-$ but becomes advantageous in our new DP method with $[Au(en)_2]^{3+}$. In contrast, the new DP method with $[Au(en)_2]^{3+}$ is considerably less efficient than the DP method with $AuCl_4^-$ in introduction of gold species on supporting oxides with high IEP values (e.g., TiO_2).[25]

Figure 2 shows the light-off curves of the activated Au catalysts supported on SBA-15, synthesized with the $Au(en)_2Cl_3$ solutions of different pH values. The results indicated that the pH value of the $Au(en)_2Cl_3$ solutions significantly affected the catalytic activity of the resulting catalysts (also see Figure 2s). Only silica-supported catalysts synthesized with the pH value of the DP solutions greater than 8.0 exhibited high catalytic activities. Clearly, the critical factor determining high catalytic activities is the nature of the solution gold species before deposition. The deprotonated DP precursor carries a positive charge of 2 instead of 3, which implies that only one outer-sphere anion is needed to maintain the neutrality when the deprotonated Au species is adsorbed on a ($Si-O^-$) surface site according to eq 2. This accompanying chloride ion can be further eliminated through the interaction of the surface complex ($[Au(en)(d\text{-}en)]^{2+}$) with a second ($Si-O^-$) surface site. After the activation of the catalysts through calcination, both gold particle size and Cl/Au mole ratio decrease with pH (Table 1), which is consistent with the above DP model. The residual chlorides on silica surfaces can poison the active sites of gold catalysts.[32] Accordingly, the lower chloride concentration introduced during the DP process can enhance both the stability and activity of the resulting catalysts. The concentrations of $[Au(en)(d\text{-}en)]^{2+}$ and surface ($Si-O^-$) both increase with pH, which further confirms the fact that the pH conditions of the DP process play a critical role in the catalytic activities of the resulting catalysts. The high pH conditions are important in the preparation of silica-supported Au catalysts with $[Au(en)_2]^{3+}$.

The structural investigations of gold nanoparticles dispersed on silica supports were performed using a HD-2000 scanning transmission electron microscope (STEM, probe size 0.3 nm) operating at 200 kV. STEM imaging with a high-angle annular dark-field (HA-ADF) detector provides higher contrast for small clusters of heavy elements in a low atomic number matrix as

TABLE 2: Representative Results of N_2 Adsorption Experiments Based on BET Calculations, Mean Diameters of Gold Particles Supported on SBA-15, and Kinetic Parameters for Oxidation of CO

sample[a,b]	surface area (m^2/g)	pore volume (cm^3/g)	average pore diameter (nm)	$T_{1/2}$ (K)	mean diameter of Au (nm)		E_a (kJ/mol)	TOF (253 K) (S^{1-})[d]
					D_{XRD}[h]	D_{TEM}[i]		
SBA-15-A-C400	559	0.92	6.5	257	3.7	4.9	17.5[e]/7.5[f]	0.45
SBA-15-A-C400-C500-1 h	–	–	–	249	3.7	–	12.7	–
SBA-15-A-C400-C500-2 h	270	0.48	6.4	237	3.9	5.2	8.0	0.84
SBA-15-A-C400-C500-3 h	–	–	–	235	3.9	–	9.0	–
SBA-15-A-C400-C500-4 h	258	0.44	6.4	246	3.9	5.1	11.1	0.65
Au/SiO_2-CVD[c]	–	–	–	227	–	6.6	17	0.02[g]

[a] A-C400: activated at 673 K. [b] C500-1 h: calcined at 773 K for 1 h in 8% O2−He. [c] From ref 20. [d] Based on the average gold size from TEM. [e] Activation energy above 253 K. [f] Activation energy below 233 K. [g] TOF (273 K). [h] D_{XRD}, Measured by XRD. [i] D_{TEM}, Observed by TEM.

compared to conventional transmission electron microscopy. The nature of the nanoparticles deposited inside the channels of SBA-15 makes these samples well-suited to HA-ADF (also known as Z-contrast) STEM imaging. Figure 3 shows the comparison of the dark-field and bright-field TEM images taken in the same location of the as-synthesized Au catalyst (reduced at 423 K in H_2/He). The HA-ADF detector in the HD-2000 subtends between 80 and 240 mrad. The bright-field image clearly illustrates that the pore structure is regular and the pore diameter is estimated to be ~70 Å. The Z-contrast imaging provides the direct proof of the presence of the Au nanoparticles uniformly dispersed on SBA-15. The key point with high-angle annular dark-field imaging is that the collection of the image is an incoherent process yielding images with strong Z (atomic number) contrast. Thus, heavy atoms (such as Au) stand out very clearly on a light background of silicon and oxygen.

The analysis of the TEM images (Figure 3) recorded for the as-synthesized catalyst reveals that the average size of the gold nanoparticles formed by the direct reduction at 423 K under H_2/He atmosphere is ~2.9 nm. Such uniformly distributed gold particles should have high catalytic activities for CO oxidation.[33] However, no catalytic activities for CO oxidation were found for the above as-synthesized catalyst without high-temperature treatment or activation. This observation indicates that the residual ethylenediamine ligands interfere with the catalytic processes through the formation of a strong bond with the surface of Au nanoparticles. The thermogravimetric analysis (TGA) of the above as-synthesized catalyst indicates that the residual ethylenediamine ligands can be mostly removed by calcination above 350 °C (see Figure 3s). The key to this high-temperature activation is to remove the ethylenediamine ligands without severe sintering induced by high-temperature calcination. Consequently, a series of experiments were conducted to determine the activation conditions. The optimum calcination temperature for activating the above catalyst system was determined to be ~673 K. The average particle size of the gold nanoparticles is ~4.9 nm, as shown in Figure 4. The activated catalyst is highly active with $T_{1/2}$ as low as 253 K, which is similar to that prepared by CVD.[8] The $T_{1/2}$ value is defined as temperature of 50% CO conversion. The average particle size is 4.9 nm.

Figure 5 shows the effect of the posttreatment at 773 K on the light-off curves and stabilities of the activated Au catalyst supported on SBA-15. The thermal stability of the activated silica-supported gold catalyst (synthesized at pH of 9.6) was studied with calcination performed at 773 K for 1−4 h in premixed 8% O_2−He (30 °C/min). As seen from Figure 5, calcination time at 773 K only has a minor effect on the activities of the activated catalyst. The reaction centers are believed to be located at the perimeter interfaces between gold and silica.[34] The minor difference in the low-temperature activities (below 233 K) can be attributed to the different degrees of the retention for carbonate species or residual organic groups.[35] As seen from Figure 5, the catalytic activity initially increases with calcination time (<3 h). This initial minor increase of the catalytic activity can be attributed to the removal of the residual organic groups. Further calcination (>3 h) can lead to a slight decrease of the catalytic activity probably because of minor sintering of the gold nanoparticles and collapse of the mesostructures. This observation indicates that the silica-supported gold catalyst is highly stable against sintering.[36] As seen from Table 2, the catalytic activity [activation energy and turnover frequency (TOF)] of the silica-supported catalyst is similar to that prepared by CVD.[20]

Mesoporous silica has a uniform size of nanopores, which can serve as an excellent support to confine nanoparticles. In addition, the mesoporous silica of SBA-15 possesses a relatively thick wall structure and therefore has a high thermal stability.[26] The stable pore-wall structure could restrain the sintering of nanoparticles without collapse of nanopores under high-temperature conditions.[37] The Z-contrast STEM images show that the activated catalysts without and with calcinations at 773 K for 1−4 h have a similar population and particle-size distribution of Au nanoparticles, as shown in Figures 6 and 7. Clearly, there was no obvious growth or sintering of the Au nanoparticles inside the nanopores of mesoporous silica during calcination. The average size of the gold nanoparticles in the activated catalyst calcined at 773 K remains close to 5.0 nm. This observation is also confirmed by the XRD study in Figure 8, which shows the XRD pattern of the activated catalyst as a function of calcination time at 773 K. The XRD patterns from calcined and uncalcined Au catalysts supported on mesoporous silica were almost identical. No significant change in the XRD line widths was observed during the calcination treatment. The gold-nanoparticle size was determined to be between 3.7 and 3.9 nm based on the peak widths in the XRD patterns (Table 2). This observation further indicates that calcination at 773 K does not significantly affect the size of the gold particles. However, calcination was found to have a significant impact on the surface areas and pore volumes of the gold catalysts (Table 2). The activated catalyst had a surface area of 559 m^2/g and a pore volume of 0.92 cm^3/g. The calcinations for 2 and 4 h resulted in the decrease of the surface area and the pore volume to 270 m^2/g, 0.48 cm^3/g, 258 m^2/g, and 0.44 cm^3/g, respectively. Clearly, part of the mesopores collapsed during calcination at 773 K. This structural collapsing could induce the formation of a porous silica coating on Au surfaces. This porous silica coating can prevent the gold nanoparicles from sintering.

Conclusion

A unique DP method for preparing highly active silica-supported Au catalysts was developed. The essence of our new DP method is to use a cationic gold precursor instead of anionic $AuCl_4^-$, and the DP process is mediated by ion-exchange

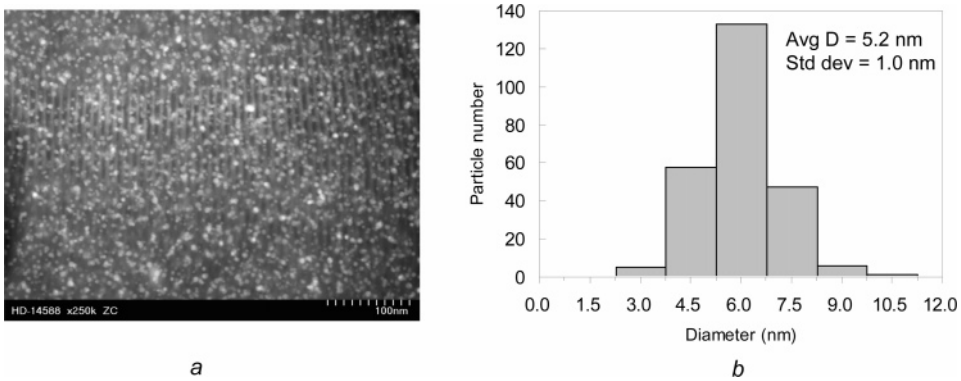

Figure 6. Dark-field TEM image (a) of the Au catalyst supported on the mesoporous silica (synthesized at pH of 9.6), which was activated at 673 K and further calcined at 773 K for 2 h after measurement of catalytic properties and the corresponding particle size distribution (b).

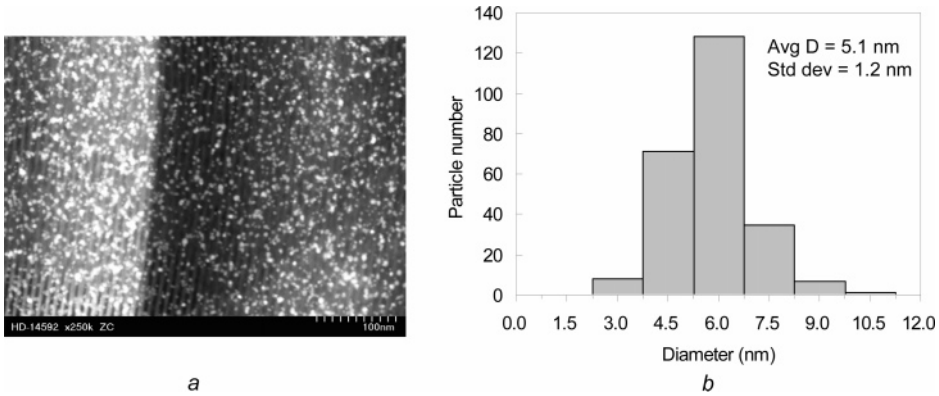

Figure 7. Dark-field TEM image (a) of the Au catalyst supported on the mesoporous silica (synthesized at pH of 9.6), which was activated at 673 K and further calcined at 773 K for 4 h after the measurement of catalytic properties and the corresponding particle size distribution (b).

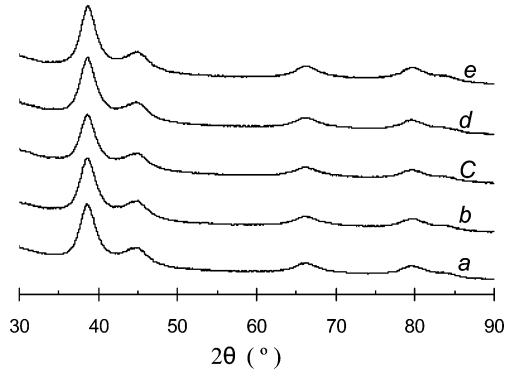

Figure 8. XRD patterns of the Au catalyst activated at 673 K (a) and further calcined in premixed 8% O_2−He at 773 K for 1 h (b), 2 h (c), 3 h (d), and 4 h (e).

processes. The pH condition of the DP solution was found to significantly affect the catalytic activities of the resulting silica-supported Au catalysts. The gold precursor can be effectively deposited on silica surfaces in the pH range between 6.0 and 10.0. The silica-supported gold catalysts prepared by the current DP method were demonstrated to be extremely stable. Most importantly, our current synthesis strategy for silica-supported gold catalysts is completely solution-based and can be applied to prepare gold catalysts supported by any kind of silica materials (e.g., silica particles and microporous zeolites).

Acknowledgment. This work was supported by the Office of Basic Energy Sciences, U.S. Department of Energy. The Oak Ridge National Laboratory is managed by UT-Battelle, LLC for the U.S. DOE under Contract DE-AC05-00OR22725. This research was supported in part by the appointments for H. Zhu to the ORNL Research Associates Program, administered jointly by ORNL and the Oak Ridge Institute for Science and Education. We would like thank the anonymous reviewers for their helpful suggestions.

Supporting Information Available: Titration curve, light-off curves, TGA analysis, and catalyst stability. This material is available free of charge via the Internet at http://pubs.acs.org.

References and Notes

(1) Haruta, M.; Kobayashi, T.; Sano, H.; Yamada, N. *Chem. Lett.* **1987**, 405.
(2) Haruta, M.; Yamada, N.; Kobayashi, T.; Iijima, S. *J. Catal.* **1989**, *115*, 301.
(3) Bond, G. C.; Thompson, D. T. *Catal. Rev.—Sci. Eng.* **1999**, *41*, 319.
(4) Kung, H. H.; Kung, M. C.; Costello, C. K. *J. Catal.* **2003**, *216*, 425.
(5) Hutchings, G. J. *Gold Bull.* **2004**, *37*, 3.
(6) Kozlov, A. I.; Kozlova, A. P.; Liu, H. C.; Iwasawa, Y. *Appl. Catal., A* **1999**, *182*, 9.
(7) Haruta, M. *CATTECH* **2002**, *6*, 102.
(8) Haruta, M. *Catal. Today* **1997**, *36*, 153.
(9) Lee, S. J.; Gavriilidis, A. *J. Catal.* **2002**, *206*, 305.
(10) Moreau, F.; Bond, G. C.; Taylor, A. O. *J. Catal.* **2005**, *231*, 105.
(11) Ivanova, S.; Petit, C.; Pitchon, V. *Appl. Catal., A* **2004**, *267*, 191.
(12) Galvagno, S.; Parravano, G. *J. Catal.* **1978**, *55*, 178.
(13) Mohr, C.; Hofmeister, N.; Lucas, M.; Claus, P. *Chem. Eng. Technol.* **2000**, *23*, 324.
(14) Chi, Y. S.; Lin, H. P.; Mou, C. Y. *Appl. Catal., A* **2005**, *284*, 199.
(15) Yang, C. M.; Kalwei, M.; Schuth, F.; Chao, K. J. *Appl. Catal., A* **2003**, *254*, 289.
(16) Overbury, S. H.; Ortiz-Soto, L.; Zhu, H. G.; Lee, B.; Amiridis, M. D.; Dai, S. *Catal. Lett.* **2004**, *95*, 99.
(17) Guczi, L.; Peto, G.; Beck, A.; Frey, K.; Geszti, O.; Molnar, G.; Daroczi, C. *J. Am. Chem. Soc.* **2003**, *125*, 4332.
(18) Martra, G.; Prati, L.; Manfredotti, C.; Biella, S.; Rossi, M.; Coluccia, S. *J. Phys. Chem. B* **2003**, *107*, 5453.
(19) Okumura, M.; Haruta, M. *Chem. Lett.* **2000**, 396.

(20) Okumura, M.; Nakamura, S.; Tsubota, S.; Nakamura, T.; Azuma, M.; Haruta, M. *Catal. Lett.* **1998**, *51*, 53.
(21) Mukherjee, P.; Patra, C. R.; Ghosh, A.; Kumar, R.; Sastry, M. *Chem. Mater.* **2002**, *14*, 1678.
(22) Zhu, H. G.; Lee, B.; Dai, S.; Overbury, S. H. *Langmuir* **2003**, *19*, 3974.
(23) Yang, C. M.; Liu, P. H.; Ho, Y. F.; Chiu, C. Y.; Chao, K. J. *Chem. Mater.* **2003**, *15*, 275.
(24) Guillemot, D.; Borovkov, V. Y.; Kazansky, V. B.; PolissetThfoin, M.; Fraissard, J. *J. Chem. Soc., Faraday Trans.* **1997**, *93*, 3587.
(25) Zanella, R.; Giorgio, S.; Henry, C. R.; Louis, C. *J. Phys. Chem. B* **2002**, *106*, 7634.
(26) Zhao, D. Y.; Feng, J. L.; Huo, Q. S.; Melosh, N.; Fredrickson, G. H.; Chmelka, B. F.; Stucky, G. D. *Science* **1998**, *279*, 548.
(27) Block, B. P.; Bailar, J. C. *J. Am. Chem. Soc.* **1951**, *73*, 4722.
(28) Mallouk, T. E.; Gavin, J. A. *Acc. Chem. Res.* **1998**, *31*, 209.
(29) Dai, S.; Burleigh, M. C.; Ju, Y. H.; Gao, H. J.; Lin, J. S.; Pennycook, S. J.; Barnes, C. E.; Xue, Z. L. *J. Am. Chem. Soc.* **2000**, *122*, 992.
(30) Makotchenko, E. V. *Russ. J. Coord. Chem.* **2003**, *29*, 720.
(31) Makotchenko, E. V.; Malkova, V. I. *Russ. J. Coord. Chem.* **2005**, *31*, 667.
(32) Oh, H. S.; Yang, J. H.; Costello, C. K.; Wang, Y. M.; Bare, S. R.; Kung, H. H.; Kung, M. C. *J. Catal.* **2002**, *210*, 375.
(33) Valden, M.; Lai, X.; Goodman, D. W. *Science* **1998**, *281*, 1647.
(34) Date, M.; Okumura, M.; Tsubota, S.; Haruta, M. *Angew. Chem., Int. Ed.* **2004**, *43*, 2129.
(35) Haruta, M.; Date, M. *Appl. Catal., A* **2001**, *222*, 427.
(36) Yan, W. F.; Mahurin, S. M.; Pan, Z. W.; Overbury, S. H.; Dai, S. *J. Am. Chem. Soc.* **2005**, *127*, 10480.
(37) Zhu, H. G.; Pan, Z. W.; Chen, B.; Lee, B.; Mahurin, S. M.; Overbury, S. H.; Dai, S. *J. Phys. Chem. B* **2004**, *108*, 20038.